ELSEVIER

Applied Surface Science 181 (2001) 149–159

applied surface science

www.elsevier.com/locate/apsusc

Chemical mapping of hot-embossed and UV-laser-ablated microchannels in poly(methyl methacrylate) using carboxylate specific fluorescent probes

Timothy J. Johnson*, Emanuel A. Waddell, Gary W. Kramer, Laurie E. Locascio

Analytical Chemistry Division, National Institute of Standards and Technology, 100 Bureau Drive, Stop 8394, Gaithersburg, MD 20899-8394, USA

Received 26 March 2001; accepted 15 June 2001

Abstract

The physical morphology and chemical functionality of fluid microchannels formed in poly(methyl methacrylate) (PMMA) substrates were studied to increase the fundamental understanding of polymer microchannel surface properties for 'lab-on-a-chip' devices. Microchannels were formed by a hot-imprint method using a silicon template or by a laser ablation process (248 nm KrF laser) operating at low to moderate fluence levels (up to 1180 mJ/cm^2). The carboxylate groups, which are responsible for the surface charges, were fluorescently labeled by reaction with an ethyl-dimethylaminopropyl-carbodiimide hydrochloride/amino-fluorescein solution. Fluorescence microscopy was then used to locate and measure qualitatively the charge present on the microchannel walls. Results suggest that surface charges are localized on the corners of trapezoidal channels formed by the hot-imprint method and that the amount of charge present is significantly less compared to laser-ablated microchannels where charges appear to be distributed uniformly. For substrates irradiated at fluences above the laser ablation threshold, it was found that one pass of the laser produced a surface with greater charge than channels made with multiple passes, that ablation under nitrogen resulted in more charge than ablation under oxygen, and that non-sonicated substrates had more charge than samples that were sonicated after ablation. Trends in the data for sonicated samples are explained through scanning electron microscopy images showing etch depth and UV-laser penetration to depths below the surface of the formed microchannel. Finally, we have determined that the surface charge on the substrate can be modified by using the laser at fluence levels lower than those required to ablate the substrate.

PACS: Microstructure — materials treatment effects 81.40; Laser ablation 79.20.D

Keywords: Carboxylate surface group; Fluorescein probe; Hot imprinting; Microchannel; Poly(methyl methacrylate); UV laser ablation

1. Introduction

Over the last decade there has been an intense focus on reducing entire laboratory systems onto microchip substrates. These systems are referred to as microscale total analytical systems (μ-TAS) or 'lab-on-a-chip' devices and often utilize micrometer-sized channels

* Corresponding author. Tel.: +1-301-975-8513; fax: +1-301-977-0587.
E-mail addresses: timothy.johnson@nist.gov (T.J. Johnson), laurie.locascio@nist.gov (L.E. Locascio).

0169-4332/01/$ – see front matter
PII: S0169-4332(01)00384-1

to transport fluids or particulates using electrokinetic [1–4], thermal [5,6], or mechanical pumping [7]. Most of the early prototype devices used photolithographic techniques and produced channels in glass or silica-based substrates because the surface properties of these materials are well characterized [8–11]. The channels were then covered with a plate of similar material [12]. Although silica-based materials have been used in successful prototype devices, the associated fabrication techniques are often difficult and/or expensive to implement.

Over the past few years a portion of the development of μ-TAS or 'lab-on-a-chip' devices has focused on the use of polymer substrates as alternative device materials because they are less expensive than silica-based substrates. Also, the availability of a wide variety of low-cost polymer materials allows for device characteristics to be tailored by simply selecting an appropriate polymer with specific chemical and/or physical traits.

Techniques for the fabrication of micrometer-sized channels in plastic substrates include molding [13], laser ablation [14], hot embossing or imprinting [15–17], X-ray lithography [18], and "soft" lithography [19,20]. Despite the success of these techniques, little is known about the surface chemistry or surface charges created during fabrication. This information is critical to the development of polymer-based 'lab-on-a-chip' devices because the most prominent form of fluid transport within the channels is electrokinetic pumping [3,4,21,22]. This phenomenon drives the fluid movement due to the interaction between the ionic content of the solution within the channel, the electric field applied between two electrodes placed within the microchannel, and the surface charge present on the channel walls [23].

For laser photoablation, there have been numerous reports offering explanations of the ablation process and the chemical mechanisms that occur. Studies have primarily focused on the ablation of poly(methyl methacrylate) (PMMA) with ultraviolet excimer lasers at 193 nm (ArF) or 248 nm (KrF) [24–32]. Unfortunately, the ablation process is complex and the exact polymer decomposition mechanism (photodegradation, thermal degradation, or a combination of the two) is still open to debate. To summarize the previous work, the ablation process using 248 nm light at a fluence in excess of the ablation threshold (typically $>0.65\ \mathrm{J/cm^2}$) produces substrates with a rough surface and ablation products consisting of methyl formate, methanol, methane, hydrogen, carbon monoxide, carbon dioxide, and solid particles with a low molecular weight fraction ($M_n = 2500$) of the original polymer ($M_n = 10^6$), which result from main chain scission [27,29,33]. An SEM image of the ejecting particles shows that they have coalesced into spheres, a sign that they have been heated beyond their melting temperature [29]. Furthermore, it has been discussed that the UV-laser light penetrates and chemically modifies the PMMA to a depth sometimes greater than the depth of ablatively removed material [34]. Finally, it has been shown that the chemical structure of PMMA can be altered even when the UV fluence is below the ablation threshold [25]. However, to our knowledge, no work has been done to investigate the residual surface charge characteristics of ablated channels in PMMA made using fluences around the ablation threshold.

There have been techniques described for using group-specific probes to map the surface charge of microchannels in polymer substrates [35,36]. Recently, our group has shown that fluorescent probes dissolved in an organic solvent can be used to detect surface groups within room-temperature imprinted channels [35]. This work showed that carboxylate groups reside primarily on the side walls of PMMA imprinted microchannels and within micro-stress cracks. While this technique was successful, it was reported that the immersion of the substrate in an organic solvent caused physical swelling and morphological changes to the imprinted channel, which could interfere with the results.

Our current study uses an aqueous fluorescence solution to map the carboxylate groups within PMMA microchannels or on the surface of PMMA substrates irradiated with a UV excimer laser (248 nm). Microchannels were formed by imprinting at elevated temperatures using a silicon template as the stamping tool, or by exposing the surface with the excimer laser above the ablation threshold. Furthermore, we compared surfaces prepared by single versus multiple laser passes and under various process conditions to study their effects on the surface charge. The results of this study should be useful for the optimization of microfluidic systems that utilize electrokinetic pumping.

2. Experimental

2.1. Reagents and materials

1-Ethyl-3-(3-dimethylaminopropyl) carbodiimide hydrochloride (EDAC, E-2247) and 5-(aminoacetamido) fluorescein (amino-fluorescein, A-1363) were obtained from Molecular Probes, Inc. (Eugene, OR). The EDAC and amino-fluorescein were dissolved in 100 mM,[1] pH 7 phosphate buffer to make a solution with a final concentration of 0.5 mM EDAC and 0.5 mM amino-fluorescein. Acrylite OP-4™ (a PMMA) was obtained from Cyro Industries (Mt. Arlington, NJ) and was used as the substrate material.

2.2. Hot imprinting method

Prior to imprinting, the PMMA substrate was cleaned with compressed air. Channels were imprinted in the substrate material using a silicon stamp with a trapezoidal-shaped raised channel [15]. The PMMA was placed over the silicon stamp, the two items were placed between two aluminum heating blocks and the temperature was raised to 110°C, and then a pressure of 5.1 MPa was applied using a hydraulic press for 1 h. The imprinted substrate was then removed, allowed to cool to room temperature, and used immediately.

2.3. Laser ablation method

A 248 nm excimer laser system (LMT-4000, Potomac Photonics, Inc., Lanham, MD) was used to surface-modify the PMMA at fluences above and below the ablation threshold. A schematic of the system is shown in Fig. 1 and contains a laser light source, a square aperture (1.164 mm × 1.164 mm) for delimiting the size and shape of the beam, a focusing lens, a visible light source, a CCD camera to image the ablation process, and a controllable X–Y stage with a vacuum chuck to hold the substrate in place. Also, a nozzle is present to sweep gas over the substrate during processing, and a vacuum is located on the opposite side to remove debris. The power level per pulse can be varied between 5 and 700 μJ, and the frequency of pulses can be set between 1 and 200 Hz, while holding the pulse width constant at 7 ns. The pulse power can be adjusted by changing the voltage applied to the laser cavity or by attenuating the beam. The average power per pulse, and corresponding standard deviation, was determined by three measurements of 100 pulses with an Energy Max 400 laser energy meter from Molectron Detector, Inc. (Portland, OR).

For the experiments conducted in this study, a square aperture was chosen such that the light after being focused exposes a 3.39×10^{-5} cm^2 area. The pulse frequency was set to 200 Hz, and the fluence was adjusted between 295 and 1180 mJ/cm^2. The standard errors of the mean for the recorded fluences ranged between 5 and 20 mJ/cm^2 for low to high fluences, respectively. The range of fluences investigated extends above and below the ablation threshold for the PMMA used here. In this study, two different sweep gases were investigated, nitrogen and oxygen, and two different UV laser exposure studies were conducted. In the first experiment, the laser was turned on, and the X–Y stage was moved linearly at a rate of 1 mm/s, exposing the PMMA over a length of 12 mm. In the second investigation, the PMMA was exposed for 12 mm in one direction, then the stage was moved in the opposite direction 12 mm, thereby exposing the same surface to the excimer laser twice.

For substrates irradiated under nitrogen, four channels were made for each fluence level of 740 mJ/cm^2 and above, and three channels were made at each fluence level below 740 mJ/cm^2. For substrates sonicated after irradiation under nitrogen, two channels were made for each fluence level of 740 mJ/cm^2 and above, and one channel was made at each fluence level below 740 mJ/cm^2. For all of the substrates irradiated under oxygen, two channels were made for each fluence level studied (1030 and 1180 mJ/cm^2). More replicate experiments were conducted at high fluence levels (>740 mJ/cm^2) due to the increased variability in the fluorescence measurements at these levels.

2.4. Fluorescence labeling and intensity measurement

The protocol used for labeling the polymer substrate microchannels with EDAC and amino-fluorescein was

[1] The accepted SI unit of concentration, mol/l, has been represented by the symbol M in order to conform to the conventions of this journal.

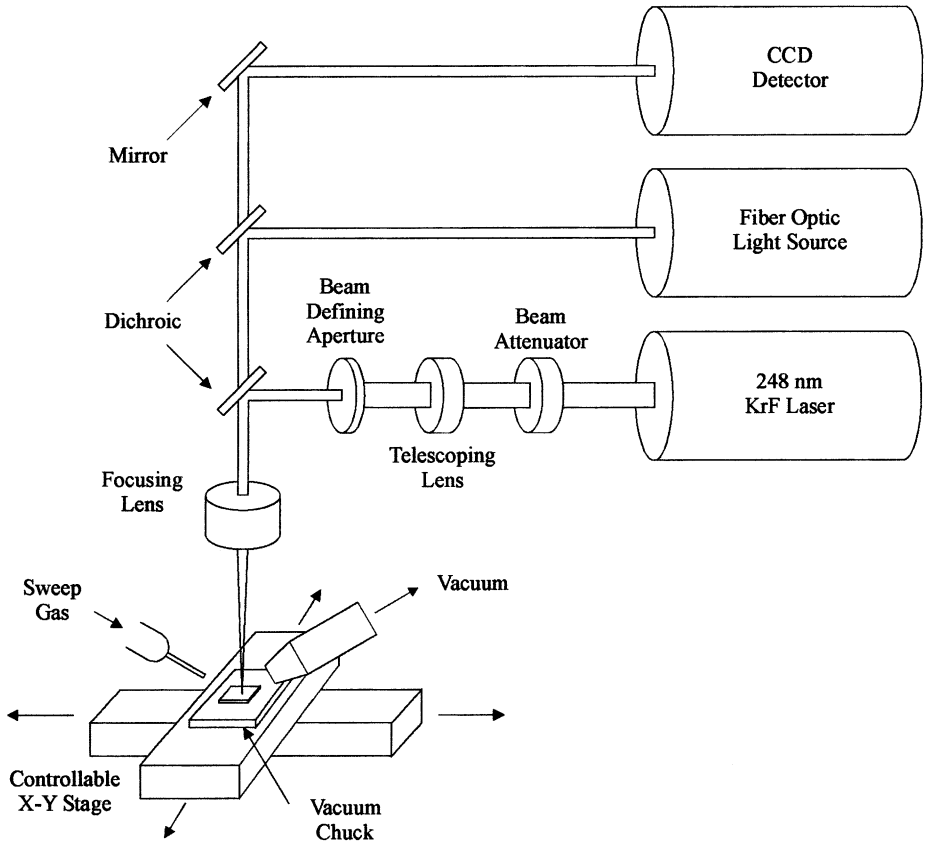

Fig. 1. Schematic of the UV-laser-photoablation system.

a modification of a previous method [37]. The EDAC was used to facilitate the reaction between the carboxylic acid surface groups of the polymer substrate and the amine group of the amino-fluorescein. This intermediate has been successfully used for probing the carboxylic acid groups of a cyclosporin derivative [38] and sugar carboxylates [39]. To label the carboxylic acid groups on the surface of the PMMA substrate, the sample was immersed in the EDAC/amino-fluorescein solution for 15 h under mild agitation. The sample was then removed and rinsed twice with 100 mM, pH 7 phosphate buffer under agitation, then rinsed twice with 138 mM, pH 9.5 carbonate buffer under agitation, followed by two final agitated rinses with the 100 mM, pH 7 phosphate buffer. The channels were then filled with the phosphate buffer under a glass coverslip and placed under the microscope. The fluorescence associated with the carboxylic acid surface charge was measured using fluorescence microscopy with a mercury lamp coupled through a bandpass filter (474–496 nm) with emission measured through a longpass filter (cutoff 530 nm), and a CCD camera for detection. Fluorescence images were taken by exposing the substrate to the mercury lamp for 1223 ms, recording the image on a personal computer, and then analyzing the image for net fluorescence intensity. Since the PMMA intrinsically fluoresces prior to EDAC/amino-fluorescein labeling, the net intensity presented in this paper is the difference between the measured intensity from the recorded fluorescence image and the background fluorescence that was measured prior to placing the sample in the EDAC/amino-fluorescein solution. The fluorescence intensity for each surface was measured, before and

after labeling, at four separate locations along the length of the irradiated surface and is reported as an average of these measurements.

3. Results and discussion

3.1. Characterization of hot imprinted channels

The dimensions of the hot-imprinted channels were measured using microscopy and optical interferometry. The trapezoidal channel was 73.2 μm wide at the top and 25.1 μm wide at the bottom with a channel depth of 31.5 μm. A white light image of the channel is shown in Fig. 2a. The imprinted channel was treated with the carboxylic-acid-specific EDAC/amino-fluorescein probe, and the resulting channel fluorescence-intensity profile is shown in Fig. 2b. The use of the aqueous EDAC/amino-fluorescein solution avoided the problems associated with polymer swelling and solvent effects seen with fluorescent labeling of substrates using a fluorescein/methanol solution [35]. The fluorescence profile in Fig. 2b was obtained by focusing on the bottom of the trapezoidal channel, and the profile was not normalized to account for the depth variation of the slanted side walls. It is difficult to ascertain the exact fluorescence distribution for the side walls because the spatial distribution of the carboxylate groups is variable and not known. Nonetheless, since the microscope was focused on the bottom of the channel, it can be said with confidence that the number of carboxylate groups is greatest at the corners of the trapezoidal channel and is distributed uniformly on the channel floor. This finding is reconfirmed by observing electrokinetic flow profiles of uncaged fluorescein molecules within an imprinted PMMA microchannel [40]. It was shown that the electroosmotic flow is greatest near the corners and bottom of the microchannel compared to the side walls.

The difference in the fluorescence profiles between this study of hot-imprinted microchannels and that of room-temperature-imprinted channels [35] is that the latter study showed, in some cases, a high degree of fluorescence along the side walls of the trapezoidal channel and essentially no fluorescence on the bottom of the channel. This can be explained by the fact that room-temperature imprinting at high pressures (55.2 MPa) creates regions of high stress with the breakage of chemical bonds in the polymer along the side-channel walls. The hot imprinting technique does not appear to induce the same degree of stress or the breaking of bonds because the polymer is heated and essentially flows away from the template to form the channel. Fig. 2b, however, shows that isolated regions of stress-induced carboxylate formation along the edges of the trapezoidal channel remain, as indicated by the high degree of fluorescence. The mean of the four fluorescence measurements taken along a single hot-imprinted channel was 190.8 arbitrary units (a.u.) with a standard error of the mean of 37.8 a.u. and is statistically similar to the inherent net fluorescence of the native PMMA material.

3.2. Characterization of laser treated substrates-fluence exposure above and below the ablation threshold

Studies were conducted with nitrogen sweep gas and laser fluences above and below the ablation threshold for PMMA. The laser ablation threshold is defined for this study as the minimal fluence level where there is noticeable mass loss or morphological change to the surface of the substrate. Fig. 3a shows a scanning electron microscopy (SEM) image for a channel made with one pass of the laser at a fluence level of 740 mJ/cm^2 (near the ablation threshold). From Fig. 3a it can be seen that there is a periodic structure, or 'ripple effect', produced on the surface of the PMMA. Microscopy images show that the periodic structure begins to occur at fluence levels near 590 mJ/cm^2 for a single pass of the laser. The periodicity of the ripples (∼5 μm) corresponds to the X–Y stage feed rate and the laser pulse frequency (1000 μm/s divided by 200 pulses/s). The lack of marking uniformity suggests a non-uniform exposure of UV light, which could be the result of overlapping pulses (the beam itself is square and 58.2 μm on a side) and/or an optical artifact in the system.

Fig. 3b and c display SEM images for the single- and two-pass channels made at 1180 mJ/cm^2 (well above the ablation threshold), respectively. It appears that there are more dark areas, or larger void spaces, in the two-pass channel compared to the single-pass channel, which may lead to a reduction in the overall surface area.

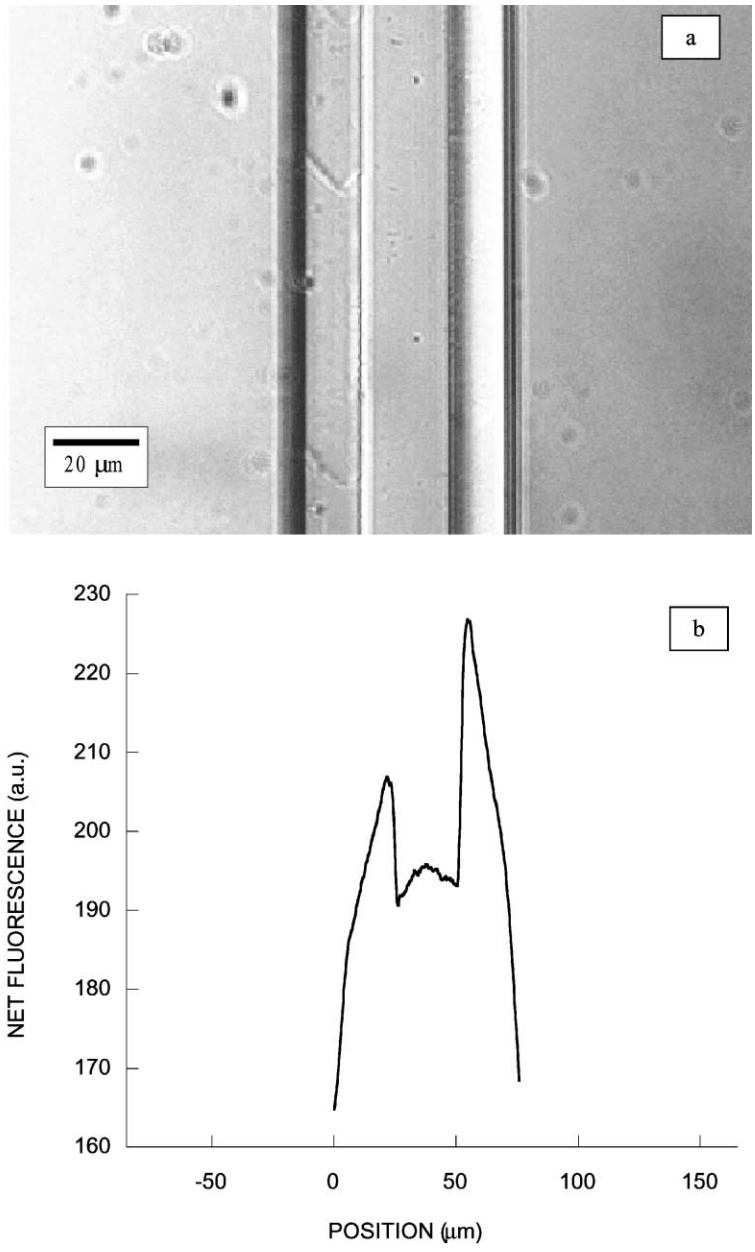

Fig. 2. (a) White light microscopy image of the trapezoidal channel formed in the PMMA by the hot-imprint method; (b) net fluorescence intensity profile of fluorescein labeled carboxylate groups on the surface of the imprinted channel.

3.3. Characterization of laser treated substrates-nitrogen sweep gas

For the experiments conducted under nitrogen sweep gas, the fluorescence due to the presence of the labeled carboxylic acid surface groups was measured as a function of the laser fluence and the numberof laser passes over the channel. The results are displayed in Fig. 4 and show that the average fluorescence intensity corresponding to the number

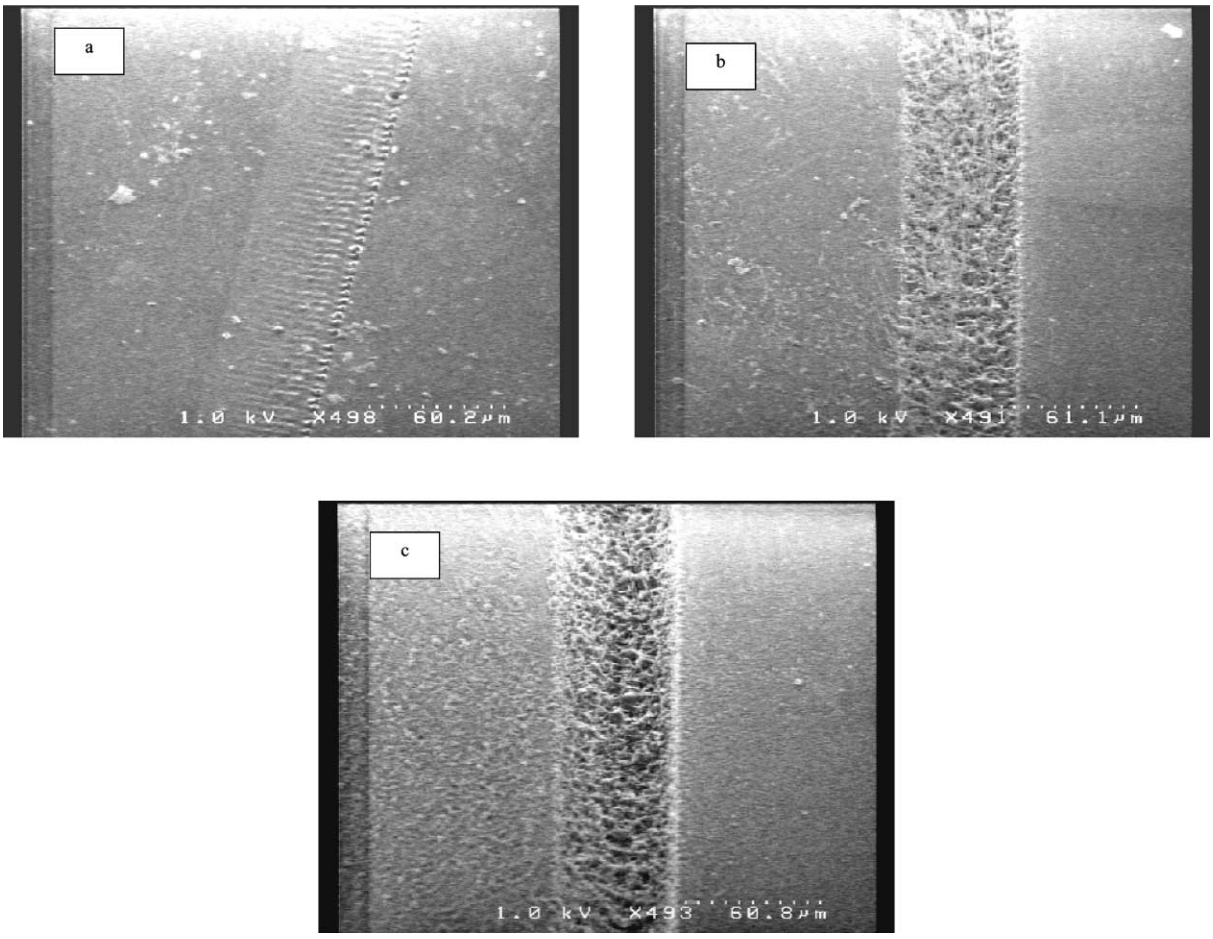

Fig. 3. (a) An SEM image of the PMMA modified by a single pass of the laser at 740 mJ/cm^2; (b) 1180 mJ/cm^2; and (c) SEM image of the ablated surface due to two passes of the laser at 1180 mJ/cm^2. All channels were made with a nitrogen sweep gas.

of carboxylate groups increases linearly until ablation begins for both one and two passes of the laser. The ablation threshold for one and two passes of the laser is 590 and 445 mJ/cm^2, respectively. Once ablation begins, the fluorescence intensity of the labeled substrates increases significantly with only moderate increases for successively higher fluences. Furthermore, it was observed that the net fluorescence, for fluences greater than the ablation threshold, was greater for channels that were exposed to the laser for one pass compared to two passes. Observation of the SEM images in Fig. 3b and c suggest that there may be a change in the surface area of the channel, although this parameter was not directly measured, but would account for the change in the magnitude of the net fluorescence for one pass of the laser compared to two.

The onset of ablation at a lower fluence level for two passes of the laser compared to one can be explained as follows. For sub-threshold ablation fluences, unsaturated species are formed on the irradiated surface of the PMMA (as detected by infrared spectroscopy), which are known to absorb more strongly in the ultraviolet as compared to non-irradiated PMMA [25]. Because of the enhanced UV absorption of the irradiated material created after one pass of the laser, PMMA can now be more easily ablated at lower fluence levels during the second pass.

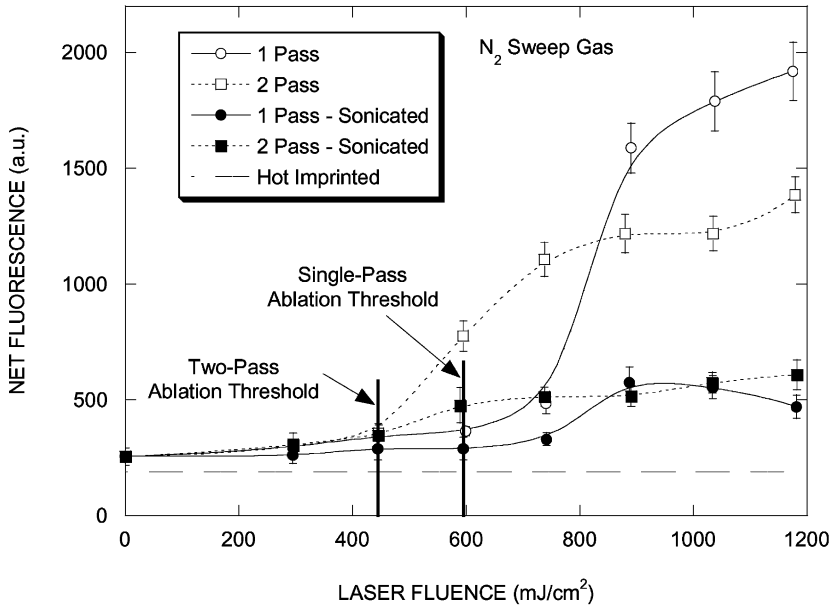

Fig. 4. Plot of the average net fluorescence intensity measured for single- and double-pass UV-exposed channels, and sonicated and non-sonicated channels made under nitrogen. The average net fluorescence intensity for the hot-imprinted channel is also shown for comparison. Error bars represent the standard error of the mean, and the curve fits are shown as an aid for observing trends in the data.

3.4. Characterization of laser treated substrates-oxygen sweep gas

Fluorescent-labeling of surface carboxylate groups was also conducted on laser-ablated channels made under oxygen. Two fluences were studied, 1036 and 1180 mJ/cm^2, and the UV laser exposed the PMMA for either one or two passes. For these experiments, the mean and the standard error of the mean of the fluorescence intensity for a single pass of the laser were 1463.4 ± 190.3 a.u. and 1425.8 ± 174.0 a.u. for fluence levels of 1030 and 1180 mJ/cm^2, respectively. For a two-pass channel, the mean and the standard error of the mean of the fluorescence intensity were 1098.6 ± 115.3 a.u. and 1014.4 ± 130.7 a.u. for fluence levels of 1030 and 1180 mJ/cm^2, respectively. Again, the average intensity for the single-pass channel is greater than the intensity for the two-pass channel; however, the respective intensities are much less than the intensities obtained from the experiments conducted under nitrogen. It has been reported that low electron affinity species, such as oxygen gas, cause a kinetic stabilization of the thermal decomposition of PMMA compared to a nitrogen gas environment [41]. Furthermore, it has been determined that the degree of stabilization increases for increased heating rates [42]. A mathematical model for UV laser ablation of PMMA suggests that the surface temperature of the substrate increases from about 400 to 700 K within 5 ns, a heating rate of 6×10^{10} K/s [43]. These surface temperatures and heating rates are within the range that oxygen gas has been shown to stabilize the thermal decomposition of PMMA [41]. It is not unreasonable to imagine that similar temperatures and heating rates occur within the ablated particles. Therefore, the stabilization of the thermal decomposition of PMMA, which prevents the formation of carboxylate groups, explains the decrease in the observed fluorescence compared to results under a nitrogen environment.

3.5. Characterization of laser treated substrates-sonicated substrates-nitrogen gas

Carboxylate-labeling experiments were conducted with laser-etched channels under a nitrogen sweep gas environment as a function of the laser fluence and the number of laser passes over the channel. After ablation

and prior to labeling the carboxylate groups, the substrate was sonicated for 5 min in a 100 mM, pH 7 phosphate buffer and then blown dry with compressed nitrogen. The substrate was then analyzed for fluorescence intensity and results are displayed in Fig. 4. From Fig. 4 it can be seen that the fluorescence intensity of the sonicated samples is significantly reduced compared to the non-sonicated substrates. This indicates that a significant amount of the charge that is created by laser ablation may reside on re-deposited material, which is removed by sonication. To show that the reduction in charge is due to the removal of re-deposited material and not due to changes in the native PMMA substrate due to sonication, Fig. 4 includes fluorescence intensity results for the native PMMA surface, sonicated and non-sonicated, prior to laser exposure (0 mJ/cm^2).

Further observance of Fig. 4 indicates that the number of carboxylate groups present on the surface of the sonicated single-pass and the two-pass channels

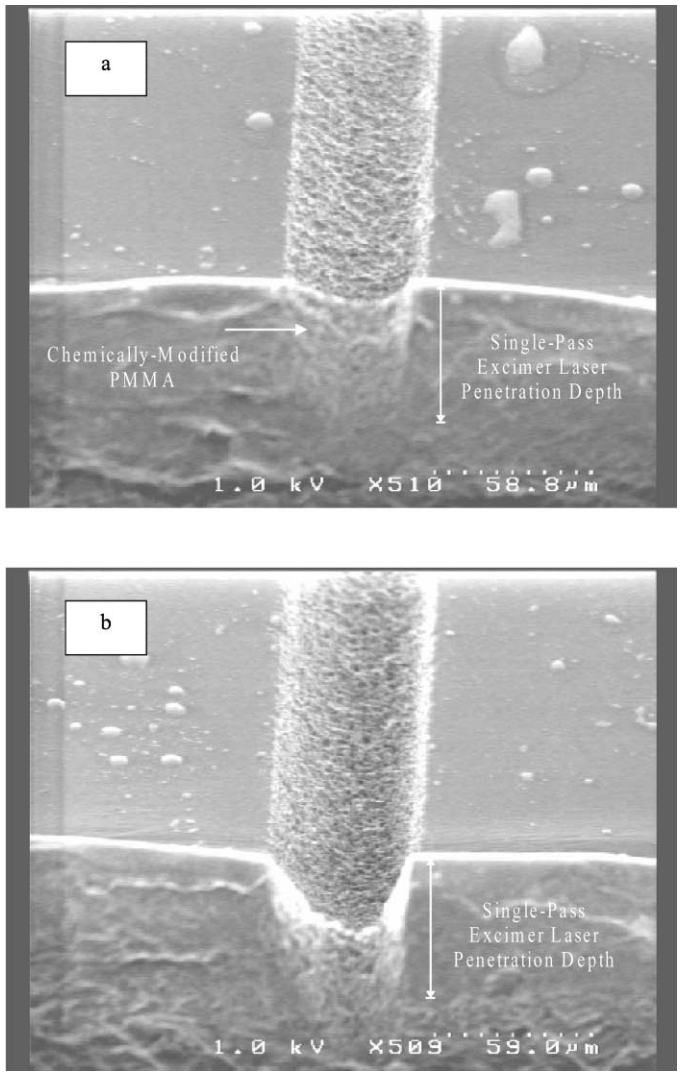

Fig. 5. An SEM cross-section image of the channels after sonication. Channels made with a fluence of 1180 mJ/cm^2, under nitrogen, and (a) one pass of the laser; or (b) two passes of the laser.

are statistically similar for fluences of 884 and 1030 mJ/cm^2. These results signify that the second pass of the laser was able to penetrate and remove the chemically modified, irradiated material on the channel surface and create a surface chemically similar to the ablation of native PMMA. However, for the highest fluence level studied, 1180 mJ/cm^2, the fluorescence intensity is greater for the two-pass sample versus the single pass. This suggests that the first pass of the laser penetrates and chemically modifies the PMMA below the channel floor, as shown in Fig. 5a, but the second pass of the laser is not able to remove all of the chemically modified, irradiated PMMA that was created during the first pass, as shown in Fig. 5b. The remaining surface of the two-pass, sonicated channel, therefore, has been exposed to the excimer laser twice, which leads to an increase in the thermal degradation and correspondingly an increase in the number of carboxylate groups compared to the single-pass, sonicated channel. Furthermore, the absence of particulates in and around the channel of Fig. 5b in comparison with Fig. 3c supports the premise that sonication removes some of the re-deposited material that was created during the ablation process.

3.6. Characterization of laser treated substrates-sonicated substrates-oxygen gas

Sonication experiments were also conducted with laser-etched channels under an oxygen sweep gas environment as a function of the laser fluence and the number of laser passes over the channel. Again, the ablated substrates were sonicated for 5 min in a 100 mM, pH 7 phosphate buffer prior to labeling and then dried with compressed nitrogen. The mean and the standard error of the mean of the recorded fluorescence intensity for a single pass of the laser was 353.0 ± 54.0 a.u. and 400.2 ± 56.4 a.u. for fluence levels of 1030 and 1180 mJ/cm^2, respectively. For a two-pass channel, the mean and the standard error of the mean of the fluorescence intensity was 478.8 ± 51.2 a.u. and 534.6 ± 40.0 a.u. for fluence levels of 1030 and 1180 mJ/cm^2, respectively. Again, the intensity is reduced significantly compared to the non-sonicated substrates produced under oxygen. Furthermore, the two-pass sample had similar average fluorescence intensities compared to the sonicated channels produced under nitrogen. The sonicated, single-pass channel had the lowest recorded intensity for these fluence levels. This trend of a reduced intensity for the single-pass channel agrees with the previous statements that oxygen gas inhibits the onset of thermal degradation of PMMA. Finally, the increase in fluorescence observed for the two-pass channels could be due to an increase in thermal degradation of the channel surface caused by the second pass of the laser. As previously discussed, at high fluences the second pass of the laser may not be able to remove all of the chemically modified, irradiated PMMA that was created during the first pass of the laser, therefore, leaving a surface that has been exposed to the excimer laser twice.

4. Conclusions

Both hot imprinting and UV laser photoablation techniques have been used to fabricate microchannels within a PMMA substrate with varying degrees of surface charge. A fluorescein probe with an intermediate binder was used to probe the carboxylate groups responsible for the surface charge within the microchannels and on surfaces irradiated below the ablation threshold. It was shown that hot-imprinted microchannels have charges that reside primarily along the bottom wall of a trapezoidal-shaped channel, whereas the surface charge can be regulated within a channel produced by UV-laser photoablation depending on the number of laser passes, the laser fluence level, and the type of sweep gas. If the fluence level is below the ablation threshold, there is no mass loss or morphological changes to the substrate, but the number of carboxylate groups is slightly increased compared to the native material — a trend that increases linearly with fluence until ablation begins. Above the ablation threshold, the number of carboxylate groups increases significantly and is higher for channels produced with a single pass of the laser compared to two passes, and for channels ablated under nitrogen compared to oxygen. Low electron affinity species, such as oxygen, stabilize the thermal degradation of PMMA [41]. Furthermore, it was found that post-ablation-sonicated samples have fewer carboxylate groups compared with non-sonicated samples, perhaps due to the removal of re-deposited particles. Also, the number of carboxylate groups generated on the surface of

post-ablation-sonicated samples has been shown to depend on the etch depth of the UV-laser light and the penetration depth of the light below the surface of the formed channel. Finally, this study suggests that UV laser photoablation can be used to create microchannels with varying wall properties.

Acknowledgements

The authors wish to acknowledge the financial support of the NRC/NIST Postdoctoral Research Program. The authors also would like to acknowledge Michael Gaitan from the Semiconductor Electronics Division at NIST for the production of the silicon templates and James Allen from the Process Measurements Division at NIST for obtaining SEM images.

References

[1] S.C. Jacobson, R. Hergenroder, A.W. Moore Jr., J.M. Ramsey, Anal. Chem. 66 (1994) 4127.
[2] K. Seiler, D.J. Harrison, A. Manz, Anal. Chem. 65 (1993) 1481.
[3] L.B. Koutny, D. Schmalzing, T.A. Taylor, M. Fuchs, Anal. Chem. 68 (1996) 18.
[4] X.C. Huang, M.A. Quesada, R.A. Mathies, Anal. Chem. 64 (1992) 967.
[5] T.K. Jun, C.-J. Kim, Tech. Dig. Solid State Sens. Actuator Workshop (1996) 144.
[6] M.A. Burns, C.H. Mastrangelo, T.S. Sammarco, F.P. Man, J.R. Webster, B.N. Johnson, B. Foerster, D. Jones, Y. Fields, A.R. Kaiser, D.T. Burke, Proc. Natl. Acad. Sci. U.S.A. 93 (1996) 5556.
[7] P. Wilding, J. Pfahler, H.H. Bau, J.N. Zemel, L.J. Kricka, Clin. Chem. 40 (1) (1994) 43.
[8] D.J. Harrison, A. Manz, Z. Fan, H. Lüdi, H.M. Widmer, Anal. Chem. 64 (1992) 1926.
[9] C.S. Effenhauser, A. Manz, H.M. Widmer, Anal. Chem. 65 (1993) 2637.
[10] S.C. Jacobson, R. Hergenröder, L.B. Koutny, R.J. Warmack, J.M. Ramsey, Anal. Chem. 66 (1994) 1107.
[11] N. Burggraf, A. Manz, E. Verpoorte, C.S. Effenhauser, H.M. Widmer, N.F. Rooij, Sens. Actuators B 20 (1994) 103.
[12] K. Fluri, G. Fitzpatrick, N. Chiem, D.J. Harrison, Anal. Chem. 68 (1996) 4285.
[13] R.M. McCormick, R.J. Nelson, M.G. Alonso-Amigo, D.J. Benvegnu, H.H. Hooper, Anal. Chem. 69 (1997) 2626.
[14] M.A. Roberts, J.S. Rossier, P. Bercier, H. Girault, Anal. Chem. 69 (1997) 2035.
[15] L. Martynova, L.E. Locascio, M. Gaitan, G.W. Kramer, R.G. Christensen, W.A. MacCrehan, Anal. Chem. 69 (1997) 4783.
[16] H. Becker, W. Dietz, P. Dannberg, in: D.J. Harrison, A. van den Berg (Eds.), Micro Total Analysis Systems 1998, Kluwer Academic Publishers, Dordrecht, The Netherlands, 1998, p. 253.
[17] L.E. Locascio, C.E. Perso, C.S. Lee, J. Chromatogr. A 857 (1999) 275.
[18] S.M. Ford, B. Kar, S. McWhorter, J. Davies, S.A. Soper, M. Klopf, G. Calderon, V. Saile, J. Microcolumn Sep. 10 (1998) 413.
[19] X.-M. Zhoa, Y. Xia, G.M. Whitesides, Adv. Mater. 8 (1996) 837.
[20] C.S. Effenhauser, G.J.M. Bruin, A. Paulus, Anal. Chem. 69 (1997) 3451.
[21] A.T. Woolley, D. Hadley, P. Landre, A.J. deMello, R.A. Mathies, M.A. Northrup, Anal. Chem. 68 (1996) 4081.
[22] L.C. Waters, S.C. Jacobson, N. Kroutchinina, J. Khandurina, R.S. Foote, J.M. Ramsey, Anal. Chem. 70 (1998) 158.
[23] J.H. Masliyah, Electrokinetic Transport Phenomena AOSTRA, Edmonton, Alta., Canada, 1994.
[24] E. Sutcliffe, R.J. Srinivasan, Appl. Phys. 60 (1986) 3315.
[25] S. Küper, M. Stuke, Appl. Phys. A 49 (1989) 211.
[26] S. Küper, S. Modaressi, M.J. Stuke, Phys. Chem. 94 (1990) 7514.
[27] R. Srinivasan, B. Braren, R.W. Dreyfus, L. Hadel, D.E. Seeger, J. Opt. Soc. Am. B 3 (1986) 785.
[28] R.J. Srinivasan, Appl. Phys. 73 (1993) 2743.
[29] R. Srinivasan, Polym. Degrad. Stabil. 43 (1994) 101.
[30] F.C. Burns, S.R. Cain, J. Phys. D Appl. Phys. 29 (1996) 1349–1355.
[31] S. Beauvois, D. Renaut, R. Lazzaroni, L.D. Laude, J.L. Bredas, Appl. Surf. Sci. 109/110 (1997) 218.
[32] R.J. Lade, I.W. Morley, P.W. May, K.N. Rosser, M.N.R. Ashfold, Diam. Rel. Mater. 8 (1999) 1654.
[33] J.F. Rabek, Polymer Photodegradation, Chapman and Hall, London, UK, 1995.
[34] R. Srinivasan, Polym. Degrad. Stabil. 17 (1987) 193.
[35] M.L. Branham, W.A. MacCrehan, L.E. Locascio, J. Cap. Electron. Microchip Technol. 1/2 (1999) 43.
[36] M.J. Wirth, M.D. Ludes, D.J. Swinton, Anal. Chem. 71 (1999) 3911.
[37] G. Hermanson, Bioconjugate Techniques, Academic Press, San Diego, CA, 1996, p. 172.
[38] P.A. Paprica, A. Margaritis, N.O. Peterson, Bioconjugate Chem. 3 (1992) 32.
[39] M. Kobayashi, Y. Chiba, Anal. Biochem. 219 (1994) 189.
[40] D. Ross, T.J. Johnson, L.E. Locascio, Anal. Chem. 73 (2001) 2509.
[41] J.D. Peterson, S. Vyazovkin, C.A. Wight, J. Phys. Chem. B 103 (1999) 8087.
[42] O.F. Shlensky, A.A. Matyukhin, E.F. Vaynshteyn, J. Therm. Anal. 31 (1986) 107.
[43] H. Schmidt, J. Ihlemann, K. Luther, J. Troe, Appl. Surf. Sci. 138/139 (1999) 102.